Supporting Information

Boosting Two-dimensional MoS_2/$CsPbBr_3$ Photodetectors via Enhanced Light Absorbance and Interfacial Carrier Separation

Xiufeng Song[†#], Xuhai Liu[†#], Dejian Yu[†], Chengxue Huo[†], Jianping Ji[†], Xiaoming Li[†], Shengli Zhang[†]*, Yousheng Zou[†], Gangyi Zhu[‡], Yongjin Wang[‡], Mingzai Wu[§], An Xie[〃], Haibo Zeng[†]*

[†]Institute of Optoelectronics & Nanomaterials, MIIT Key Laboratory of Advanced Display Materials and Devices, College of Materials Science and Engineering, Nanjing University of Science and Technology, Nanjing 210094, China.

E-mail: zeng.haibo@njust.edu.cn, zhangslvip@njust.edu.cn

[‡]Grünberg Research Centre, Nanjing University of Posts and Telecommunications, Nanjing 210003, China.

[§]School of Physics and Materials Science, Anhui University, Hefei 230601, P.R.China.

[〃]Key Laboratory of Functional Materials and Applications of Fujian Province, College of Materials Science and Engineering, Xiamen University of Technology, Xiamen 361024, P.R.China.

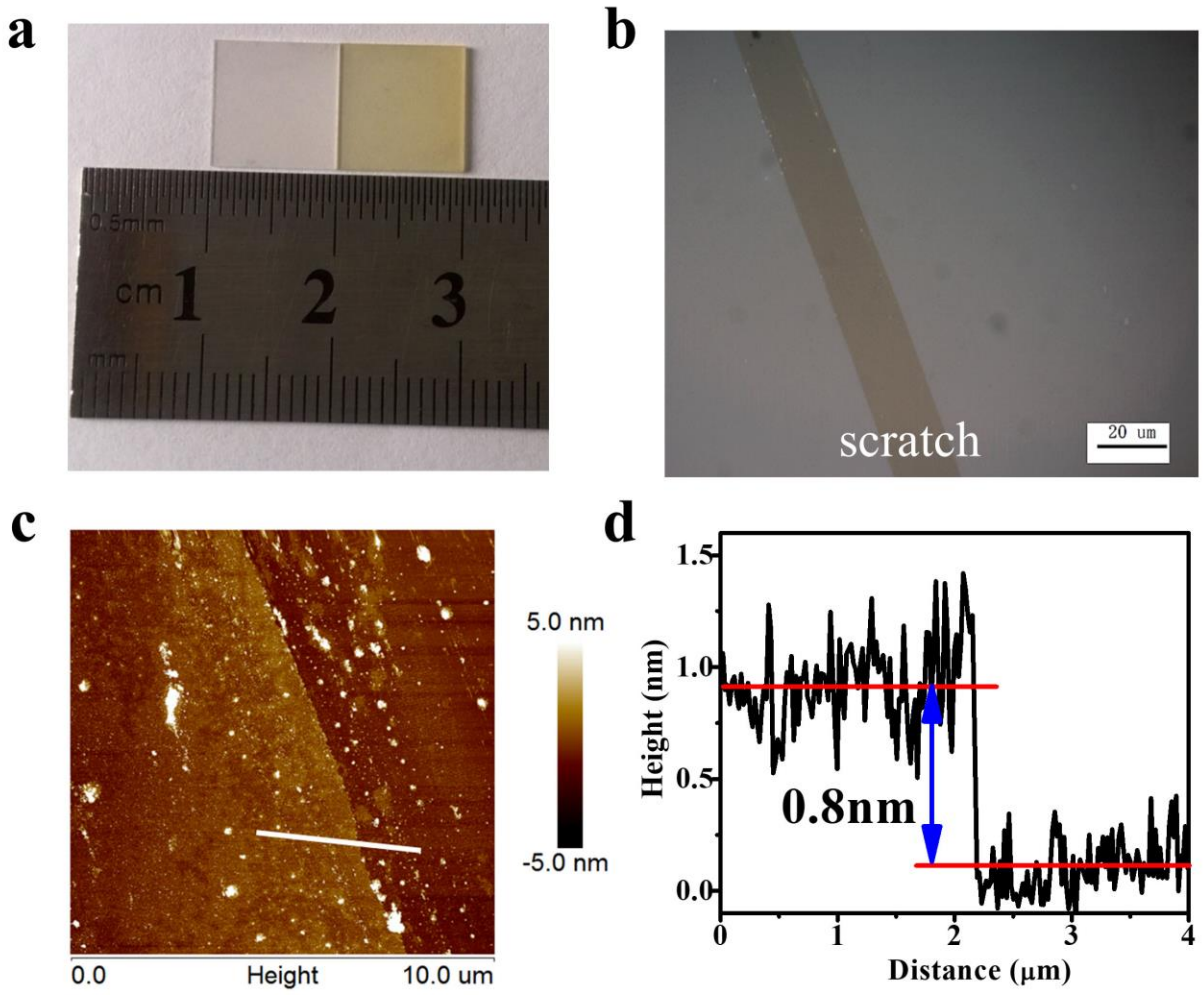

Figure S1. Large-area uniformity of the synthesized MoS_2 film. a) Photograph of as-grown MoS_2 monolayer, left: bare sapphire substrate, Right: fully covered MoS_2 monolayer on sapphire substrate. b) Optical image of the MoS_2 monolayer. c) AFM image of the obtained MoS_2 monolayer. d) Height profile corresponding to the white line shown in c).

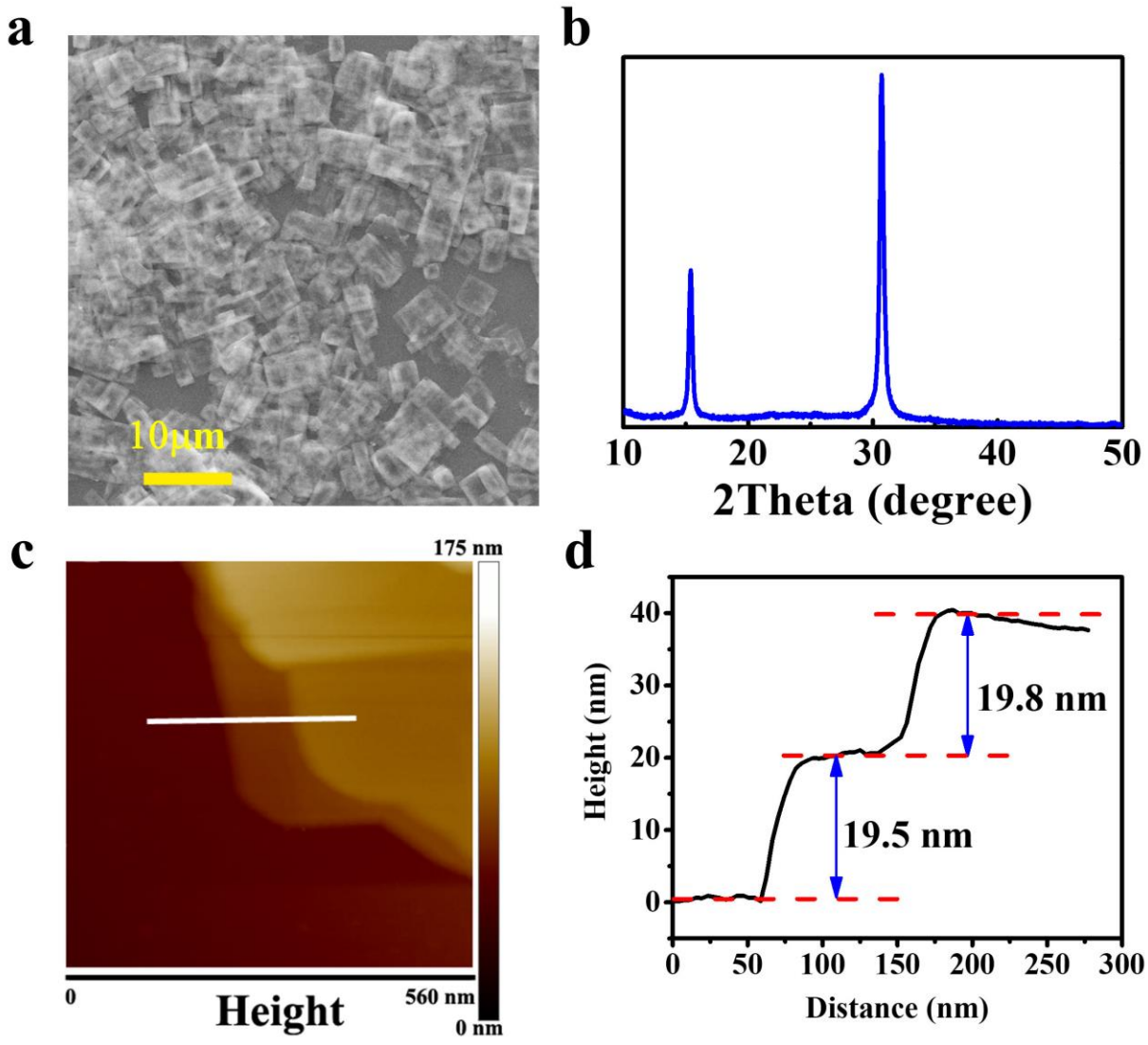

Figure S2. a) SEM image and b) XRD pattern of the $CsPbBr_3$ nanosheets. c) AFM image of the obtained $CsPbBr_3$ nanosheets. d) Height profile for the white line shown in c).

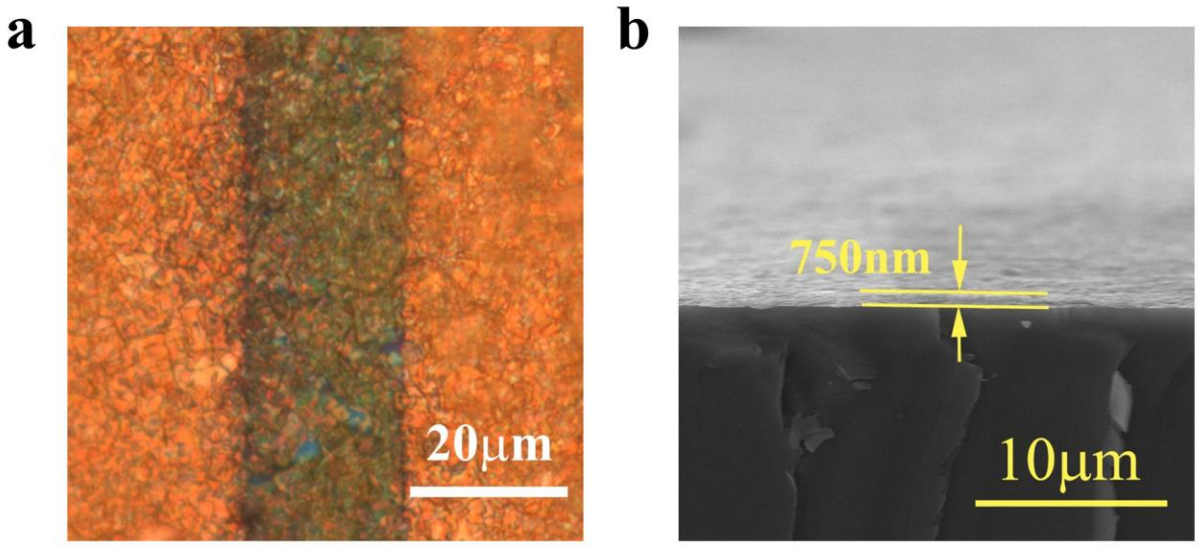

Figure S3. a) Optical image of the hybrid MoS_2/$CsPbBr_3$ photodetector. b) Cross-sectional SEM image of the coated CsPbBr3 nanosheets.

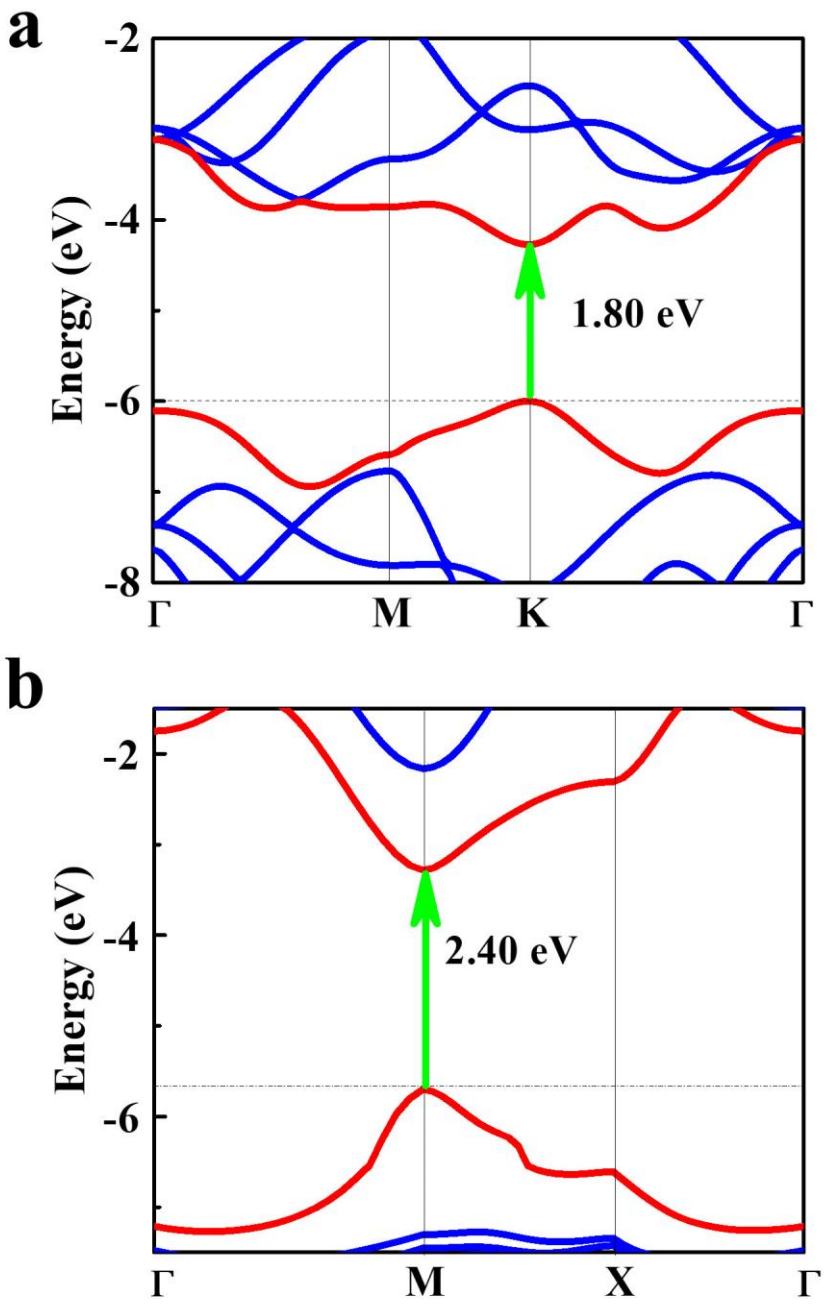

Figure S4. Calculated band structure of a) MoS_2 and b) $CsPbBr_3$.

Our calculated results (MoS_2 with band gap 1.8 eV, and $CsPbBr_3$ with band gap 2.4 eV) agree well with those experimentally determined values[S1-3].

PL lifetime of pure $CsPbBr_3$ and $MoS_2/CsPbBr_3$ perovskite structure

Figure 3b shows the time-resolved PL decay transients measured at 515 nm for pure $CsPbBr_3$ and hybrid $MoS_2/CsPbBr_3$.

The experimental curves of the PL decay could be fitted well using the biexponential functions:

$$A(t) = A_0 + A_1 * exp\left(\frac{-t}{\tau_1}\right) + A_2 * \exp\left(\frac{-t}{\tau_2}\right) \quad \text{(S1)}$$

The average lifetime (τ) is calculated from

$$\tau = \frac{\sum A_i \tau_i^2}{\sum A_i \tau_i} \quad \text{(S2)}$$

Table S1. PL lifetimes of $CsPbBr_3$ and $MoS_2/CsPbBr_3$.

	A_1	τ_1 (ns)	A_2	τ_2 (ns)	R^2	τ (ns)
$CsPbBr_3$	5.70	2.06	0.81	13.33	0.987	7.46
$MoS_2/CsPbBr_3$	30.54	1.42	0.66	4.99	0.992	1.67

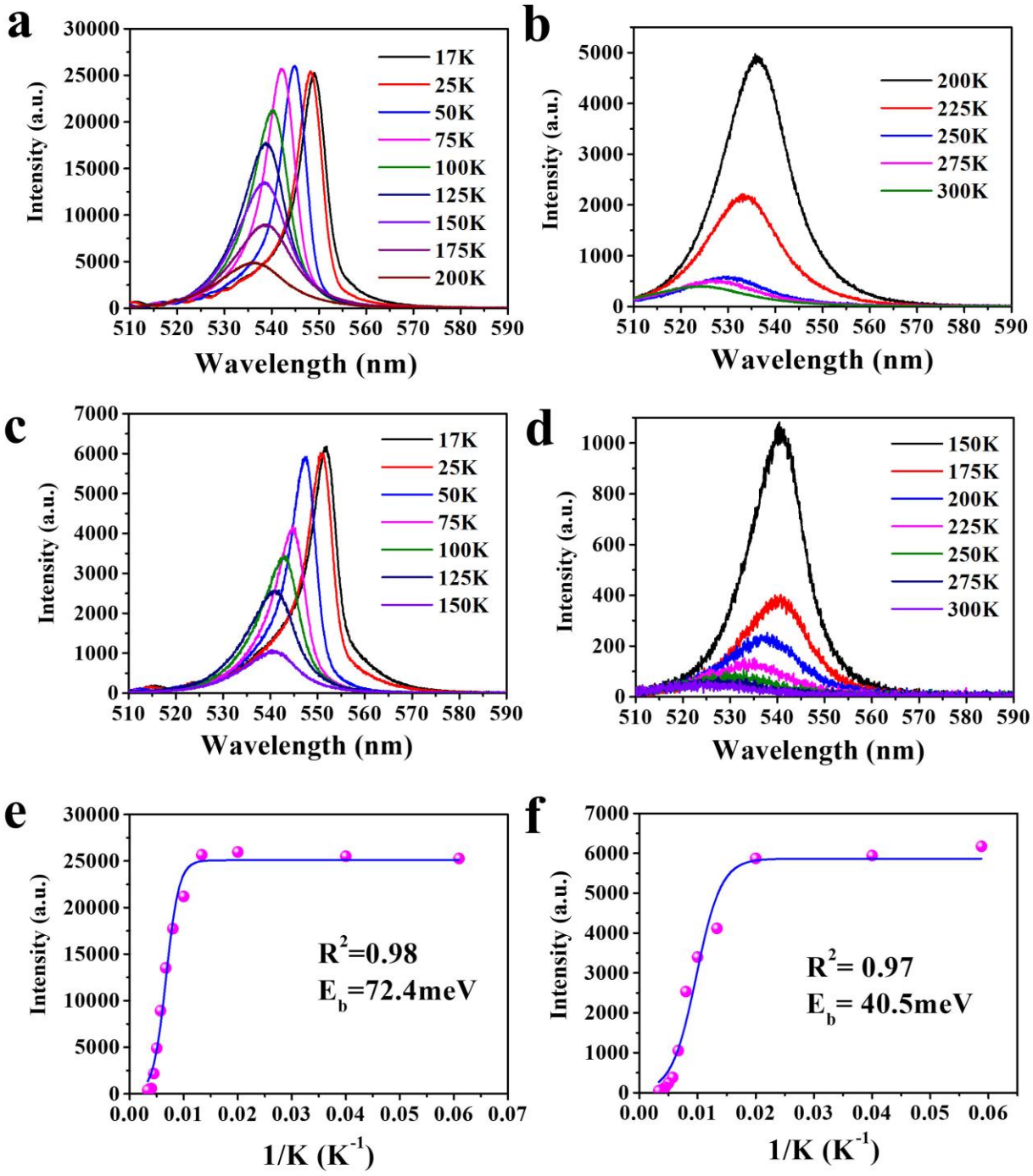

Figure S5. Temperature dependent PL spectra of a),b) $CsPbBr_3$, and c),d) $MoS_2/CsPbBr_3$. (e) Temperature dependent PL intensity of $CsPbBr_3$. f) Temperature dependent PL intensity of $MoS_2/CsPbBr_3$.

As shown in Figure S5, the PL intensity of the $CsPbBr_3$ can decrease with increasing the temperature. The exciton binding energy can be calculated by the following equation:

$$I(T) = \frac{I_0}{1+Ae^{-E_b/k_bT}} \quad \text{(S3)}$$

where, I_0 is the PL intensity at 0 K, k_b is the Boltzmann constant, E_b is the exciton binding energy. The calculated exciton binding energy of $CsPbBr_3$ and $MoS_2/CsPbBr_3$ are 72.4 meV and 40.5 meV, respectively. The decrease of the exciton binding energy indicates that the generated excitons in the hybrid structure tend to separate more easily during the device operation process, which is beneficial to increase the photocurrent of the photodetector based on $CsPbBr_3/MoS_2$.

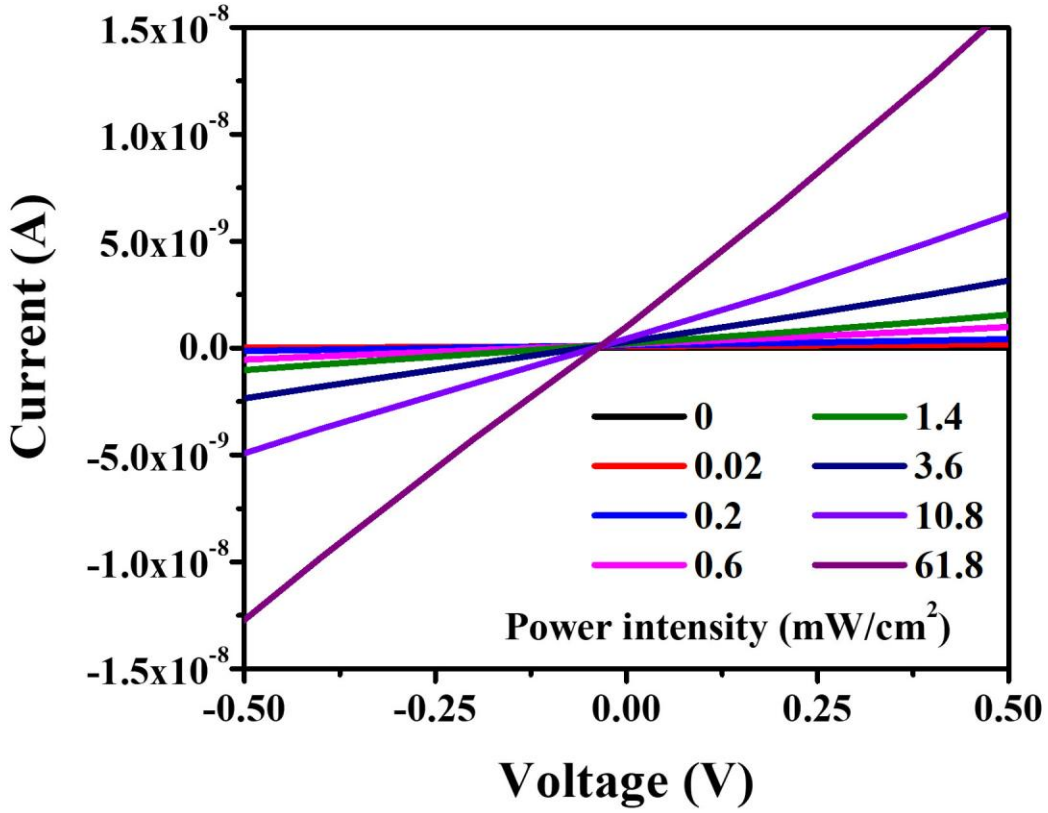

Figure S6. Drain-source characteristic of $MoS_2/CsPbBr_3$ device in the darkness and under different illumination intensities.

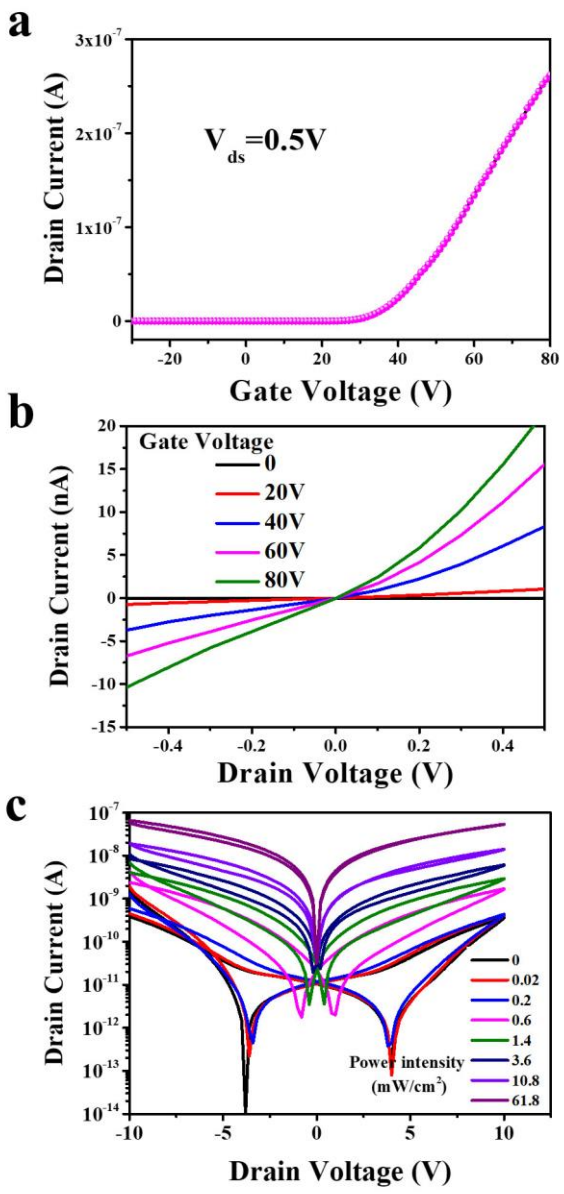

Figure S7. Electrical characteristics of MoS_2 transistor. a) Transfer characteristics. b) Output characteristics with different gate voltage. c) Drain-source characteristic in darkness and under different illumination intensities.

Due to the wet-transfer process, water or organic residues could exist on the surface of MoS_2 and at the MoS_2/SiO_2 interface, leading to the reduction of conductivity and large hysteresis of the devices. This is in consistence with previous reports in literature.[S4-6]

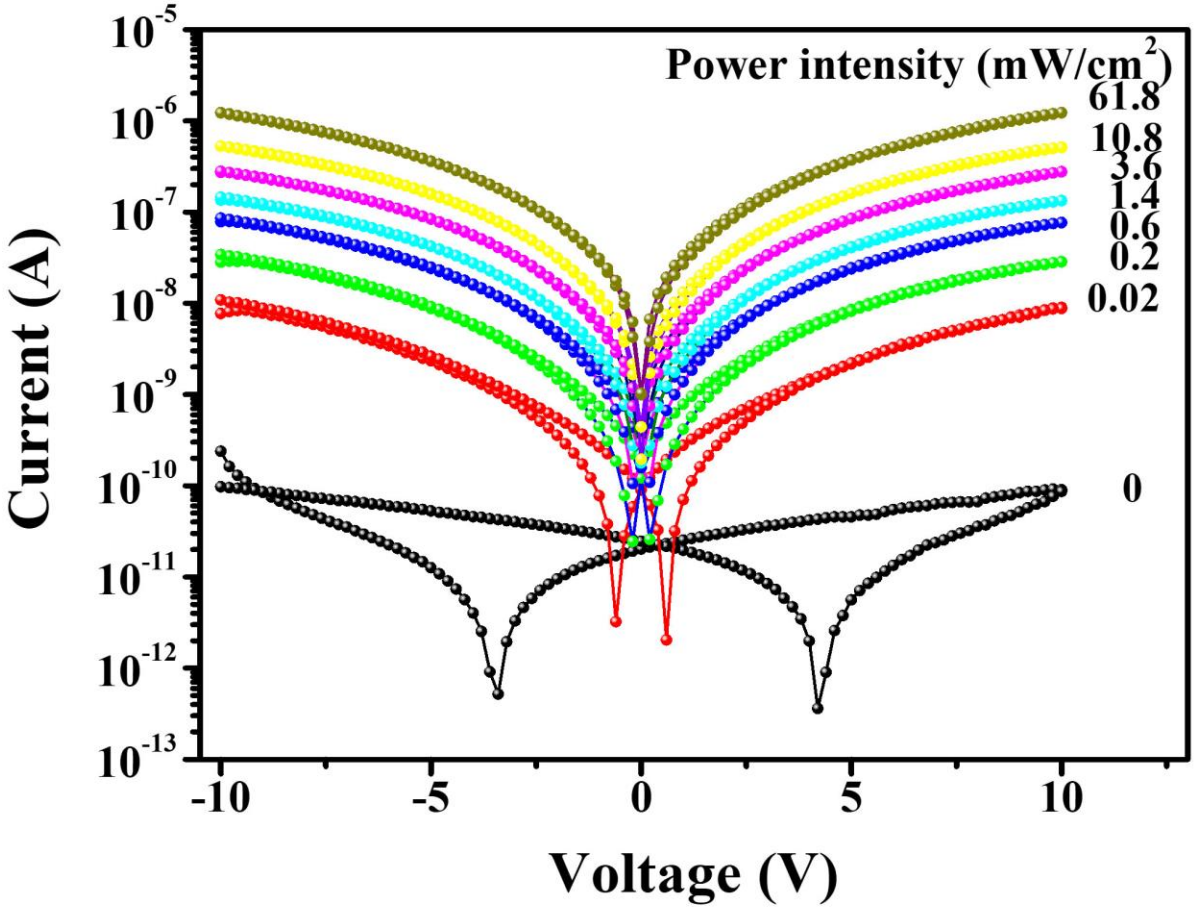

Figure S8. Drain-source characteristic of $CsPbBr_3$ photodetector in darkness and under different illumination intensities.

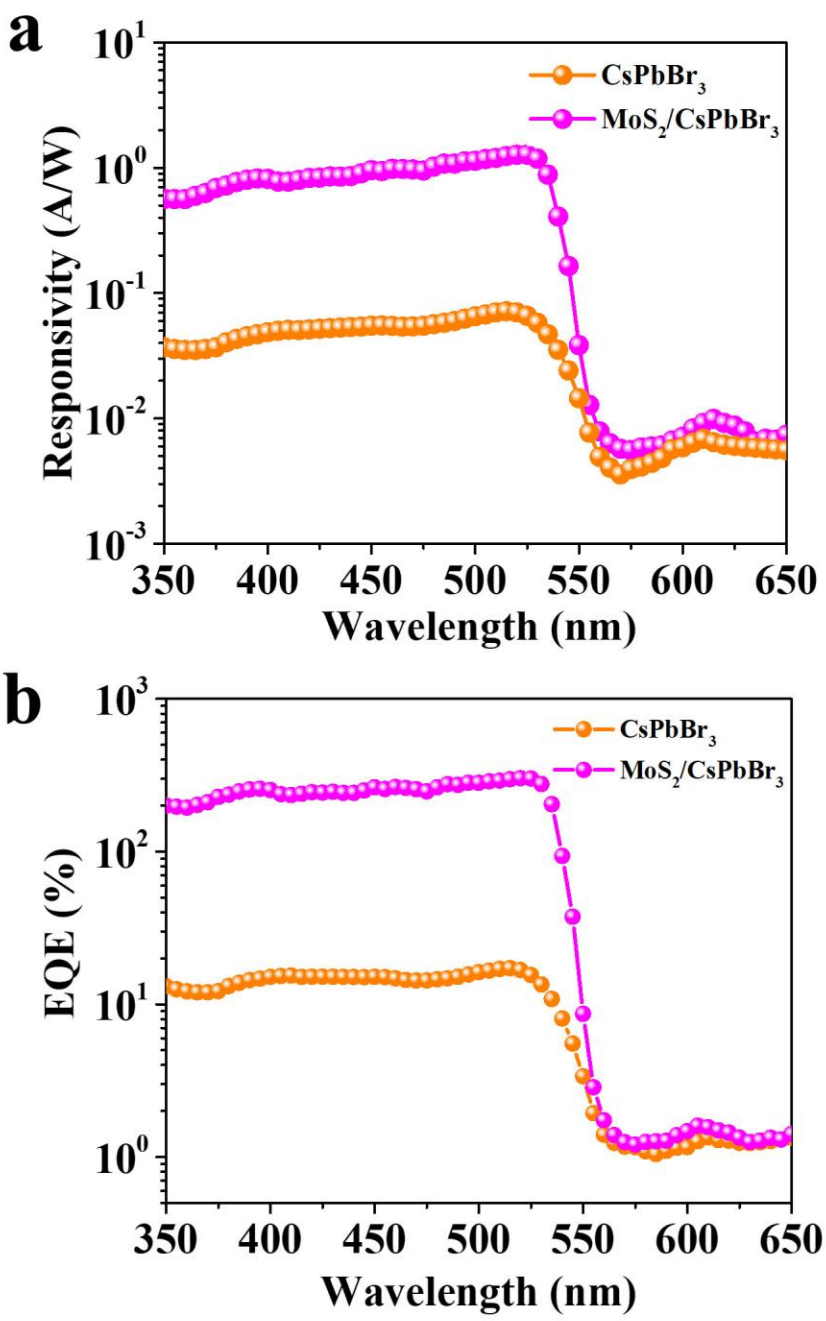

Figure S9. a) Photoresponsivity and b) EQE of $CsPbBr_3$ photodetectors with or without MoS_2 as a function of illumination wavelength.

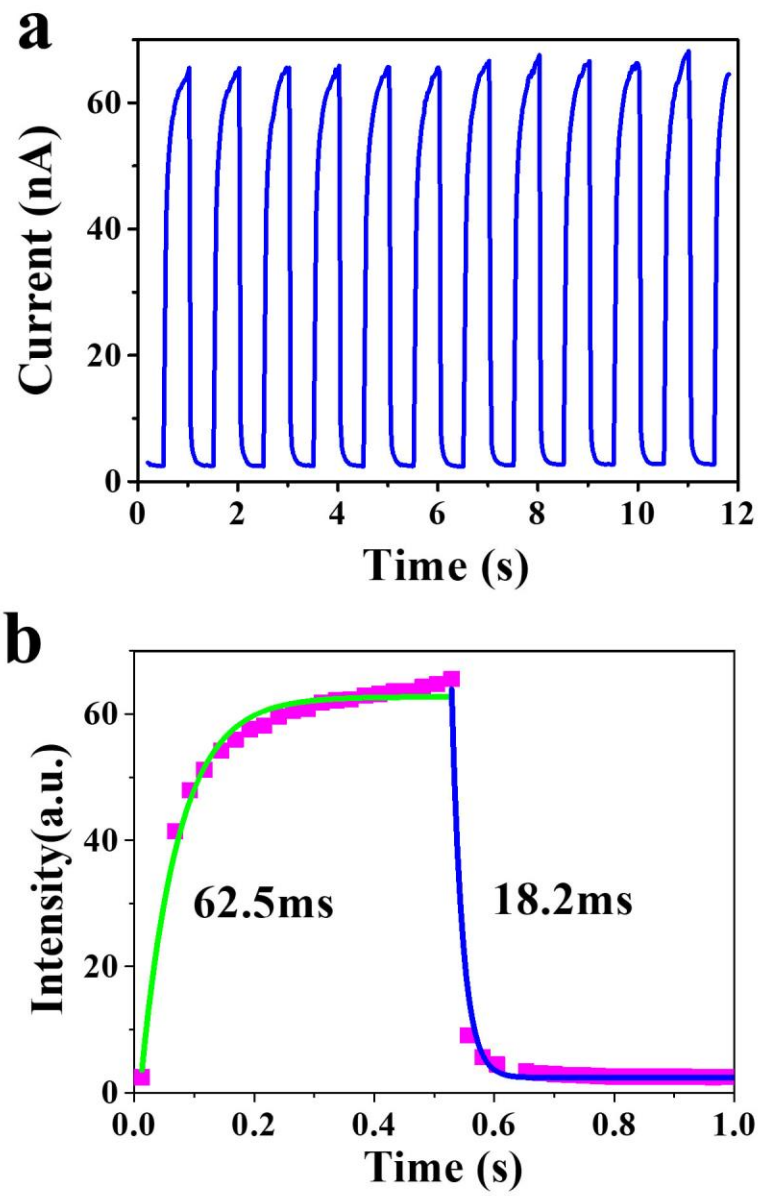

Figure S10. Time-resolved photoresponse of the $CsPbBr_3$ photodetector under 442 nm laser illumination. a) Photoswitching behavior of the hybrid device at different voltages and incident optical power intensity. b) Temporal photocurrent response of the hybrid device with rising time (62.5 ms) and decay time (18.2 ms).

Table S2. Performance comparing of photodetectors on 2D/Perovskite.

Device structure	Incident	Responsivity (A/W)	Detectivity (J)	Rise /fall	Ref.
MoS_2	150pW @561nm	880		4s /9s	S7
MoS_2	4mW cm^{-2} @633nm	0.12	10^{11}	-	S8
WSe_2	10nW @532nm	0.15	-	-	S9
InSe	0.66 mW cm^{-2} @405nm	12.3	5.47×10^{10}	50ms /60ms	S10
$CH_3NH_3PbI_3/MoS_2$/APTES	4.63pW @520nm	2.11×10^{4}	1.38×10^{10}	6.17s /4.5s	S11
$CH_3NH_3PbI_3$/1T-MoS_2	0.14mW @500nm	3.3×10^{5}	7×10^{11}	0.45s /0.75s	S12
$CH_3NH_3PbI_3$/2H- MoS_2	0.14mW @500nm	142	2.6×10^{11}	25ms /50ms	S12
$MAPbI_3$/Graphene	3.3 pW @633nm	2.6×10 6	-	55s /75s	S13
$CH_3NH_3PbI_3$/Graphene	0.002 mW @515nm	115	3×10^{12}	-	S14
$CH_3NH_3PbPbBr_2I$/Graphene	223 μW @405nm	6.0×10^{5}	-	120ms /750ms	S15
$CH_3NH_3PbI_3/WSe_2$	70 mW cm^{-2} @532nm	1.1×10^{5}	2.2×10^{12}	2.1s /3s	S16
$CH_3NH_3PbI_3$/Graphene	1 μW @520nm	180	10^{9}	87ms /540ms	S17
$CsPbBr_{3-x}I_x$/Graphene	0.07 mW cm^{-2} @405nm	8.2×10^{8}	2.4×10^{16}	0.81s /3.65s	S18
$CH_3NH_3PbI_3/WS_2$	0.2 μW cm^{-2} @505nm	17	2×10^{12}	2.7ms /7.5ms	S6
$CsPbBr_3$	4.65 mW cm^{-2} @532nm	0.00471	16.84×10^{8}	0.2 ms /1.3 ms	S2
$CsPbBr_3$/Au	4.65 mW cm^{-2} @532nm	0.01004	4.56×10^{8}	0.2 ms /1.2 ms	S2
$CsPbBr_3/MoS_2$	20μW cm^{-2} @442nm	4.4	2.5×10^{10}	0.72ms /1.01ms	This work

References in Supporting Information:

S1. Mak, K. F.; Lee, C.; Hone, J.; Shan, J.; Heinz, T. F., Atomically Thin MoS_2: A New Direct-Gap Semiconductor. *Phys. Rev. Lett.* **2010,** *105* (13), 136805.

S2. Dong, Y.; Gu, Y.; Zou, Y.; Song, J.; Xu, L.; Li, J.; Xue, J.; Li, X.; Zeng, H., Improving All-Inorganic Perovskite Photodetectors by Preferred Orientation and Plasmonic Effect. *Small* **2016,** *12* (40), 5622-5632.

S3. Kulbak, M.; Cahen, D.; Hodes, G., How Important Is the Organic Part of Lead Halide Perovskite Photovoltaic Cells? Efficient $CsPbBr_3$ Cells. *J. Phys. Chem. Lett.* **2015,** *6* (13), 2452-2456.

S4. Late, D. J.; Liu, B.; Matte, H. S. S. R.; Dravid, V. P.; Rao, C. N. R., Hysteresis in Single-Layer MoS_2 Field Effect Transistors. *ACS Nano* **2012,** *6* (6), 5635-5641.

S5. Li, T.; Du, G.; Zhang, B.; Zeng, Z., Scaling behavior of hysteresis in multilayer MoS_2 field effect transistors. *Appl. Phys. Lett.* **2014,** *105* (9), 093107.

S6. Ma, C.; Shi, Y.; Hu, W.; Chiu, M.-H.; Liu, Z.; Bera, A.; Li, F.; Wang, H.; Li, L.-J.; Wu, T., Heterostructured $WS_2/CH_3NH_3PbI_3$ Photoconductors with Suppressed Dark Current and Enhanced Photodetectivity. *Adv. Mater.* **2016,** *28* (19), 3683-3689.

S7. Lopez-Sanchez, O.; Lembke, D.; Kayci, M.; Radenovic, A.; Kis, A., Ultrasensitive photodetectors based on monolayer MoS_2. *Nat. Nanotechnol.* **2013,** *8* (7), 497-501.

S8. Choi, W.; Cho, M. Y.; Konar, A.; Lee, J. H.; Cha, G.-B.; Hong, S. C.; Kim, S.; Kim, J.; Jena, D.; Joo, J.; Kim, S., High-Detectivity Multilayer MoS_2 Phototransistors with Spectral Response from Ultraviolet to Infrared. *Adv. Mater.* **2012,** *24* (43), 5832-5836.

S9. Pradhan, N. R.; Ludwig, J.; Lu, Z.; Rhodes, D.; Bishop, M. M.; Thirunavukkuarasu, K.; McGill, S. A.; Smirnov, D.; Balicas, L., High Photoresponsivity and Short Photoresponse Times in Few-Layered WSe_2 Transistors. *ACS Appl. Mat. Interfaces* **2015,** *7* (22), 12080-12088.

S10. Tamalampudi, S. R.; Lu, Y.-Y.; Kumar U, R.; Sankar, R.; Liao, C.-D.; Moorthy B, K.; Cheng, C.-H.; Chou, F. C.; Chen, Y.-T., High Performance and Bendable Few-Layered InSe Photodetectors with Broad Spectral Response. *Nano Lett.* **2014,** *14* (5), 2800-2806.

S11. Kang, D.-H.; Pae, S. R.; Shim, J.; Yoo, G.; Jeon, J.; Leem, J. W.; Yu, J. S.; Lee, S.; Shin, B.; Park, J.-H., An Ultrahigh-Performance Photodetector based on a Perovskite–Transition-Metal-Dichalcogenide Hybrid Structure. *Adv. Mater.* **2016,** *28* (35), 7799-7806.

S12. Wang, Y.; Fullon, R.; Acerce, M.; Petoukhoff, C. E.; Yang, J.; Chen, C.; Du, S.; Lai, S. K.; Lau, S. P.; Voiry, D.; O'Carroll, D.; Gupta, G.; Mohite, A. D.; Zhang, S.; Zhou, H.; Chhowalla, M., Solution-Processed MoS_2/Organolead Trihalide Perovskite Photodetectors. *Adv. Mater.* **2016,** *29* (4), 1603995.

S13. Spina, M.; Lehmann, M.; Náfrádi, B.; Bernard, L.; Bonvin, E.; Gaál, R.; Magrez, A.; Forró, L.; Horváth, E., Microengineered $CH_3NH_3PbI_3$ Nanowire/Graphene Phototransistor for Low-Intensity Light Detection at Room Temperature. *Small* **2015,** *11* (37), 4824-4828.

S14. Dang, V. Q.; Han, G.-S.; Trung, T. Q.; Duy, L. T.; Jin, Y.-U.; Hwang, B.-U.; Jung, H.-S.; Lee, N.-E., Methylammonium lead iodide perovskite-graphene hybrid channels in flexible broadband phototransistors. *Carbon* **2016,** *105*, 353-361.

S15. Wang, Y.; Zhang, Y.; Lu, Y.; Xu, W.; Mu, H.; Chen, C.; Qiao, H.; Song, J.; Li, S.; Sun, B.; Cheng, Y.-B.; Bao, Q., Hybrid Graphene–Perovskite Phototransistors with Ultrahigh Responsivity and Gain. *Adv. Optical Mater.* **2015,** *3* (10), 1389-1396.

S16. Lu, J.; Carvalho, A.; Liu, H.; Lim, S. X.; Castro Neto, A. H.; Sow, C. H., Hybrid Bilayer WSe_2–$CH_3NH_3PbI_3$ Organolead Halide Perovskite as a High-Performance Photodetector. *Angew. Chem. Int. Ed.* **2016,** *55* (39), 11945-11949.
S17. Lee, Y.; Kwon, J.; Hwang, E.; Ra, C.-H.; Yoo, W. J.; Ahn, J.-H.; Park, J. H.; Cho, J. H., High-Performance Perovskite–Graphene Hybrid Photodetector. *Adv. Mater.* **2015,** *27* (1), 41-46.
S18. Kwak, D.-H.; Lim, D.-H.; Ra, H.-S.; Ramasamy, P.; Lee, J.-S., High performance hybrid graphene-$CsPbBr_{3-x}I_x$ perovskite nanocrystal photodetector. *RSC Adv.* **2016,** *6* (69), 65252-65256.